Astron. Astrophys. 322, 159–166 (1997)

ASTRONOMY AND ASTROPHYSICS

H_2O maser emission from irregular variables⋆

M. Szymczak[1] **and D. Engels**[2]

[1]Toruń Radio Astronomy Observatory, Nicolaus Copernicus University, ul. Gagarina 11, PL-87100 Toruń, Poland
[2] Sternwarte der Universität Hamburg, Gojenbergsweg 112, D-21029 Hamburg, Germany

Received 31 July 1996 / Accepted 13 November 1996

Abstract. We have performed a search for the 22 GHz water maser line among 72 optically identified irregular and semiregular red variables. New detections were made of five stars, while only four of nine objects previously known as maser sources were redetected. The probability for the detection of H_2O maser emission increases with V light amplitude, and with $H-K$ and $K-[12]$ colours just as in regular Mira and semiregular variables of SRa– and SRb–types. The detection rate of water masers is about 25% for nearby Lb objects (D <400 pc) in the sample, comparable to that observed in the SRa and SRb stars. No masers were detected in objects with mass loss rates $\leq 4\,10^{-8} M_{\odot}\mathrm{yr}^{-1}$. Maser luminosities are $10^{41}-10^{43}$ photons s^{-1} similar to that of the bluest Miras and typical SRa and SRb stars showing water maser emission. A comparison of our data on irregular stars with those previously obtained on SRa and SRb variables suggests that most radio and infrared properties are indistinguishable among both classes of objects.

Key words: masers – stars: circumstellar matter – stars: mass-loss – stars: AGB, post-AGB – radio lines: stars

1. Introduction

Water maser emission from the $6_{16} \rightarrow 5_{23}$ transition is characteristic of an oxygen–rich environment which is common in M–giants and related objects with considerable mass loss. More than half of an IRAS colour selected sample of 382 OH/IR stars show water masers (Engels & Lewis 1996). Bowers & Hagen (1984) have estimated that about 75% of the Mira variables in the solar neighbourhood ($\leq$400 pc) have associated H_2O masers with a luminosity $\geq 10^{41}$ photons s^{-1} at maximum light. In a sample of northern ($\delta > -20°$) SRa and SRb semiregular variables having about the same distance range about 20% were detected (Szymczak & Engels 1995). All of these objects exhibit more or less regular pulsational behaviour. Besides them, many M−type objects with irregular optical light curves of small amplitudes (usually $1-2^{\mathrm{m}}$ in V) are known, the so called Lb and SR stars (Kholopov et al. 1985–88). Although some of them are presumably misclassified Miras or semiregulars due to insufficient variability data, it is likely that they form an intrinsic group. The nature and causes of their pulsational behaviour as well as their evolutionary status are poorly understood. The chaotic behaviour of the V light curve might be due to multimode pulsation (Jura & Kleinmann 1992) or interaction between the fundamental mode and an overtone mode when the object is close to dynamical instability (Buchler & Goupil 1988). Recently, Jura & Kleinmann (1992) have considered irregulars as progenitors of Miras and semiregulars with periods of 300−400 days and 100−150 days, respectively.

Irregular stars have not reached the popularity as much as Miras in observational radio studies. Data on masers in these objects are very scarce (Benson et al. 1990). In collisionally pumped water masers the mass loss rate is one of the essential factors controlling the strength of the emission (Cooke & Elitzur 1985), and there is observational evidence that the detection rate as well as the luminosity of the masers depend on the mass loss rate (Bowers & Hagen 1984; Lewis & Engels 1993). Because the infrared colours of most of the irregulars are typical for mass losing objects, probably also the oxygen–rich irregulars with signs of circumstellar envelopes are sites of water emission. The purpose of the present investigation was to search for the 22 GHz water line in a sample of irregular stars, to derive the properties of their masers and to compare them with those of other late–type stars of different pulsational behaviour. Preliminary results were reported by Szymczak (1996).

2. Observations

The sample consists of 72 objects selected originally from the printed release of the General Catalogue of Variable Stars (Kholopov et al. 1985–88, GCVS), which are classified as Lb– or SR–type variables there. In the tape version of the GCVS most of the SR–type variables are reclassified as SRa (N=2) and SRb (N=17) semiregular variables. Our objects match the following criteria: (1) $\delta > -20^0$, (2) spectral type is M. For all but one star a third condition $K-[12] > 1.25$ is obeyed.

Send offprint requests to: M. Szymczak

⋆ Table 2 is only available electronically at CDS via anonymous ftp 130.79.128.5

Here, the apparent magnitudes at K were taken from Gezari et al. (1993), and [12] is the zero point corrected magnitude at IRAS 12 μm band as found in the explanatory supplement to the IRAS PSC (IRAS Science Team, 1988).

The $6_{16} \rightarrow 5_{23}$ maser line of H_2O at 22235.08 MHz was observed with the 100 m Effelsberg radio telescope during three sessions in 1995 March 26–27, June 23–24 and September 18–19. A single channel K–band maser receiver installed in the primary focus of the telescope was used. The system noise temperature was 90–200 K depending on weather conditions and elevation angle, and the beamwidth (FWHP) was 42″. The spectrometer was a 1024 channel three–level autocorrelator for which a bandwidth of 25 MHz provided a velocity coverage of $\pm$160 km s $^{-1}$ relative to the LSR. This bandwidth was used for the search of new masers. The total–power position switching mode was used with on–source integration times of 2 minutes. With this set–up the 3 σ detection level is $\sim$0.6 Jy. Part of the detected objects were reobserved with 5 minutes integration time and a bandwidth of 6.25 MHz. The spectra have a velocity resolution of 0.33 km s $^{-1}$ at 25 MHz and of 0.16 km s $^{-1}$ at 6.25 MHz after Hanning smoothing.

The observations were centred on the IRAS positions. Regular pointing checks and data calibration were made using the continuum sources NGC7027, 3C286 and Mon R2. All spectra were corrected for the average atmospheric attenuation and elevation dependent gain variations of the telescope. The absolute flux calibration has an accuracy of about 20%.

3. Results

The H_2O maser detections are presented in Table 1. For each star the name, the variable type, the coordinates, the peak velocities $V_{\rm p}$ and fluxes $S_{\rm p}$, the velocity interval ΔV of the maser emission and the integrated flux $S_{\rm i}$ are given. Water masers were detected for the first time in CE And, BX Eri, VZ Eri, CW Cnc and V2090 Oph. The maser spectra of the detected stars are displayed in Figure 1.

The two newly discovered variables CE And and BX Eri with emission peaks of 22.5 and 40.1 Jy, respectively, are the strongest sources besides TU Lyr. Their spectra show a highly asymmetric pattern with a peak at each edge of the emission velocity range of width 11.6 and 8.3 km s^{-1}, respectively. A similar spectrum is observed for TU Lyr with the strongest peak at $\sim$7 km s^{-1}, which diminished in intensity by 30% over a 3 month interval. Its double-peaked spectrum is completely reversed in intensity as compared with a spectrum taken in 1988 July when the strongest peak was at 2.7 km s^{-1} (Engels, unpublished Effelsberg data). Five sources have maser spectra composed of a single feature or few features extending over $<$4 km s^{-1} with the flux density of the most prominent peak usually less than 1.5 Jy. The discovery of V2090 Oph is remarkable because it shows maser emission over a velocity interval of 27.5 km s^{-1}, which is unusual for irregular and semiregular variables. This object was first detected in 1995 June as rather weak maser source with the strongest peak of 1.7 Jy at $-$27 km s^{-1}. The integrated emission of this source increased by a factor of 4.2 in 3 months and new features appeared.

The undetected stars are listed in Table 2 with their common and IRAS names, the variable type, the dates of observations and the 3σ upper limit for the peak flux emission. Some of them such as T Psc, BK Vir, WY Boo and TY Dra were detected in 1988–1991 (Engels, unpublished Effelsberg data). TW Peg was detected by Dickinson (1976).

4. Analysis

4.1. Statistics of water masers

The originally selected sample has become inhomogeneous in terms of variability type due to improvements in classification of several stars in the tape version of the GCVS. The analysis of H_2O maser properties in irregular variables will be restricted therefore to the 46 Lb–type variables in the sample. The reclassified SR–type variables were added to the sample of SRa- and SRb-type variables studied by Szymczak & Engels (1995), to serve as comparison sample. The few remaining SR variables may turn out as SRa and SRb objects as well when the light curves are better sampled. For now, they are not further considered. Also QS Her (SRb) and V2090 Oph (Lb:) are not included in the following analysis as they are probably misclassified as well (see below). The 5 objects already known as masers but not redetected in the present observations, likely due to strong variability, are considered as maser sources.

Of the 45 Lb stars in total, 6 are H_2O maser sources. In the comparison sample of semiregulars (now N = 115 objects), 30 are associated with maser emission. Thus, the detection rate in irregulars is about a factor of two lower than among semiregulars. However, as will be discussed below, this is due to a selection effect.

The visual amplitudes of the Lb stars in the sample are in general less than $2\overset{\rm m}{.}0$, with 82% of them having an amplitude $< 1\overset{\rm m}{.}5$. Although the V amplitude may be inaccurately determined due to a bad coverage of the light curve and possible temporal variations, we find a general trend that the probability of water maser detection increases with visual amplitude (Fig. 2). In 19 objects with amplitudes $\leq 1\overset{\rm m}{.}0$ only one source was detected, while for larger amplitudes the rate raises to 19%.

29 Lb stars in our sample have spectra in the LRS IRAS catalogue (IRAS Science Team, 1986). The majority of them belong to classes 1n and 2n, only one object is of 4n spectral type. The LRS class distribution for the sample is shown in Fig. 3. For the 3 featureless (LRS class 10–14) objects, no maser was detected, while one object was detected among the 15 LRS class 1n objects in the range 15–19. For stars of LRS classes 20–24 and 25–29 about half of the stars are maser sources. No maser was detected in the 4n type object. It follows that the presence of water maser emission is strongly correlated with the LRS class 2n, which designates spectra showing a silicate feature at 10 μm.

A histogram of the $K - [12]$ colour distribution for the Lb variables is shown in Fig. 4. The irregulars are restricted to a

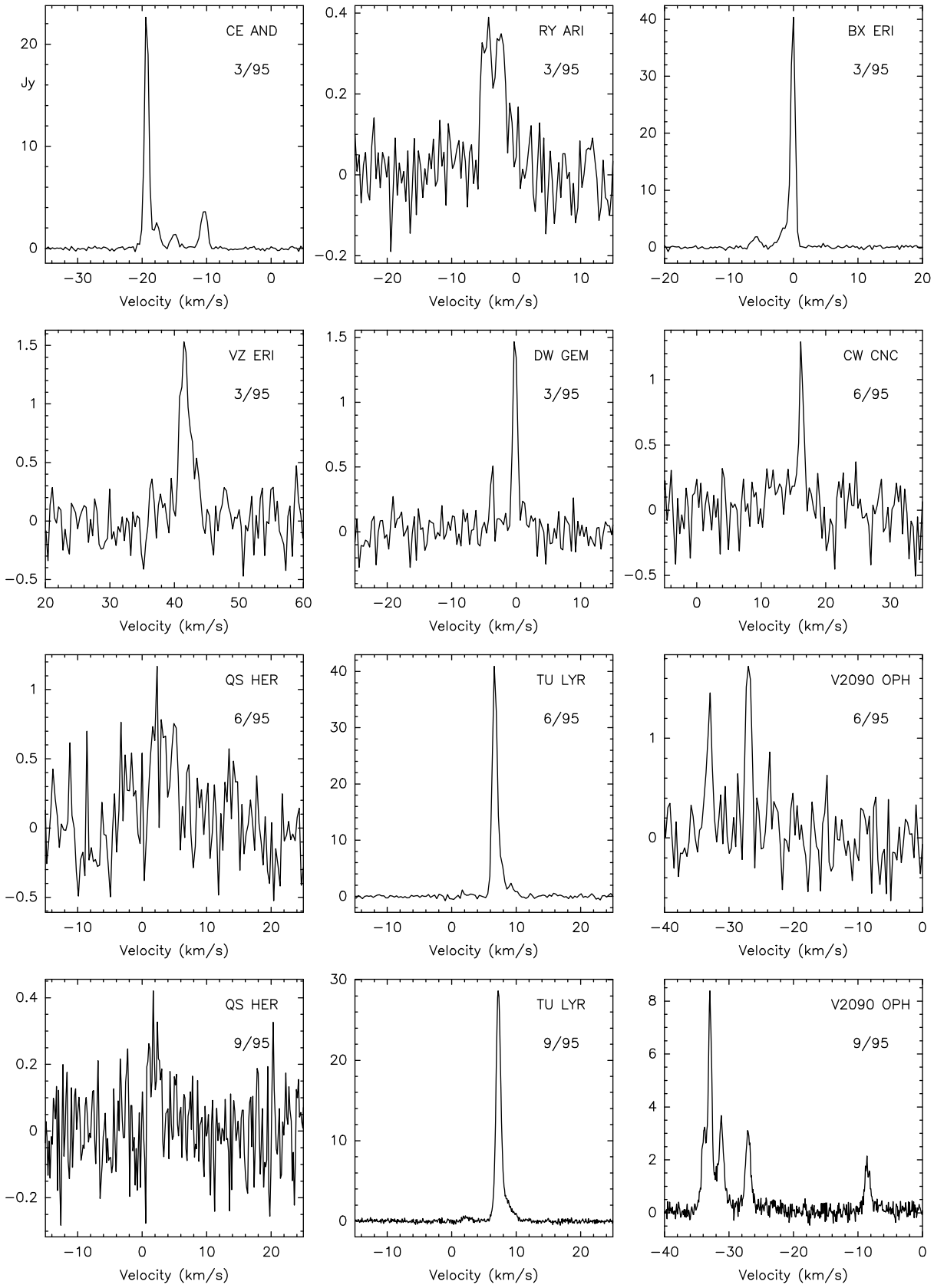

Fig. 1. Spectra of the 22 GHz H_2O masers in irregular and semiregular giants.

Table 1. Irregular and semiregular stars with H_2O maser emission

Name	Var. type	α(1950) (h m s)	δ(1950) (° ′ ″)	Obs. date	V_p (km s^{-1})	S_p (Jy)	ΔV (km s^{-1})	S_i (10^{-22}Wm^{-2})
CE And[a]	Lb	01 26 33.5	46 24 07	3/95	−19.4	22.5	11.6	218
					−17.8	2.5		
					−15.0	1.3		
					−10.4	3.5		
RY Ari	Lb	01 59 45.9	16 01 52	3/95	−6 – −2	0.4		<10
BX Eri[a]	SR	04 38 14.8	−14 17 47	3/95	−5.8	1.7	8.3	321
					−1.6	3.5		
					0.0	40.1		
VZ Eri[a]	SR	04 39 23.3	−08 02 59	3/95	41.5	1.5		24
DW Gem	Lb	06 27 51.4	27 29 16	3/95	−3.8	0.5		16
					−0.1	1.4		
				6/95		<0.7		
CW Cnc[a]	Lb	09 05 42.1	13 25 23	6/95	16.2	1.3		15
QS Her	SRb	18 07 37.0	34 45 40	6/95	∼2	1.2		∼ 26
				9/95	1.9	∼0.4		<10
TU Lyr	Lb	18 18 37.6	31 43 54	6/95	2.3	∼1.0		337
					6.6	40.8		
					9.2	2.3		
				9/95	2.1	∼0.5	∼9.6	236
					7.3	28.6		
V2090 Oph[a]	Lb:	18 21 22.9	03 35 43	6/95	−32.9	1.5		35
					−27.0	1.7		
				9/95	−33.8	3.2	27.5	150
					−32.9	8.4		
					−31.3	3.7		
					−27.0	3.1		
					−8.6	2.1		

[a] new detection

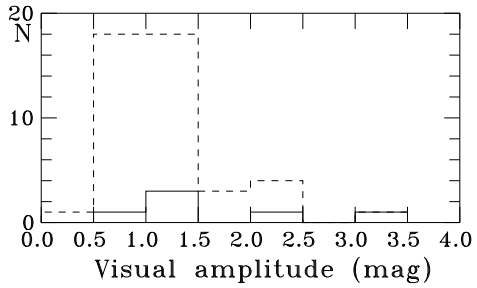

Fig. 2. Distribution of visual amplitude in the observed sample of irregular stars (dashed line). The solid line refers to maser stars.

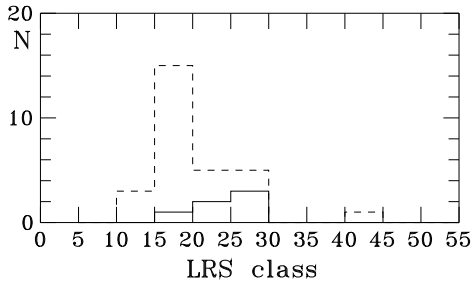

Fig. 3. Histogram of LRS classes of irregular objects (dashed line). The solid line refers to maser stars.

very narrow colour range with 93% of the objects having $1.25 < K - [12] < 2.0$. The detection rate of water masers increases with colour, a trend seen also for SRa and SRb variables and Miras (Szymczak 1996). Furthermore, the Lb objects of the present sample and the SRa/SRb stars of the comparison sample share almost the same colour range and they appear to be an extension of Miras towards bluer colours with a partial overlap of these classes (Szymczak 1996).

The presence of water maser emission among irregular variables is therefore linked to the presence of a silicate emission feature and redder infrared colours. The $K - [12]$ colour, which is a measure of the relative fluxes from the star and from the dust envelope, is tightly correlated with the mass loss rate for cool stars (Whitelock et al. 1994). We therefore argue that maser emission is sustained among those few irregular stars which have well developed circumstellar envelopes due to mass loss at significant rates. Because the variability type classification in the GCVS is frequently based on incomplete observations, a misclassification cannot be excluded. The irregular variable stars with well developed circumstellar shells could then be intrinsic semiregular or even Mira variables, as well. It is therefore the presence of significant mass loss in an oxygen-rich star,

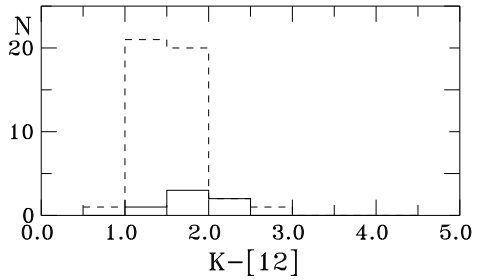

Fig. 4. Distribution of $K - [12]$ colour of the Lb stars (dashed line). The solid line refers to maser stars.

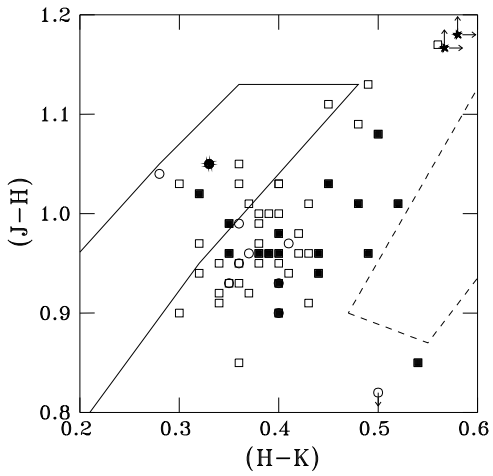

Fig. 5. NIR two colour diagram for the Lb stars (circles). A subset of SRa and SRb variables (squares) are included for comparison. The water maser stars are marked by filled symbols. The loci of non-variable normal giants (solid contour) and of Mira variables (dashed contour) are given after Whitelock et al. (1994). The outliers (stars) in the upper right corner are QS Her and V2090 Oph.

which determines the occurrence of water masers. The variability type, e.g. the pulsational properties, are linked to water maser presence only because high-amplitude variables have in general larger mass-loss rates than variables with smaller amplitudes.

4.2. Comparison with other cool stars

To study in more detail the nature of the irregular stars with associated H_2O maser emission, a subsample of 10 Lb objects and a comparison subsample of 52 SRa and SRb objects with $JHKLM$ photometry available (Fouqué et al. 1992; Gezari et al. 1993; Kerschbaum & Hron 1994; Whitelock et al. 1995) have been extracted. The near–infrared (NIR) two colour diagram for these stars is shown in Fig. 5. One Lb star and 17 SRa/SRb stars are H_2O emitters. The average domains of the normal late–type giants and of Mira variables are also indicated. The irregulars share the near-infrared properties of SRa and SRb variables and bridge the gap between the normal non-variable giants and Mira variables. QS Her and V2090 Oph are clearly outside of the irregular and semiregular domain. Their NIR colours strongly suggest that they are OH/IR stars or Mira variables. QS Her

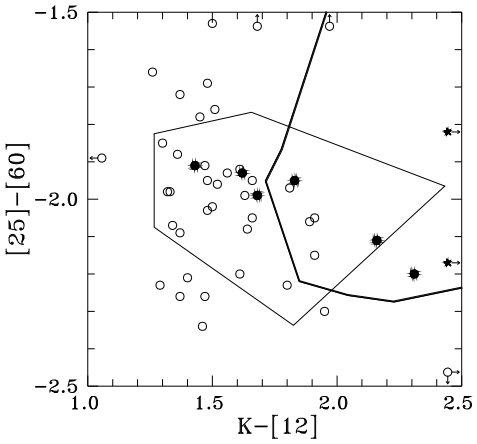

Fig. 6. Diagram of the IRAS [25]−[60] colour versus $K - [12]$ colour for the stars studied. The masers are marked with filled circles and non-maser stars with open circles. The thin line contour displays the domain of the SRa and SRb water maser variables in the comparison sample. The right hand area delineated by thick line is occupied by all Mira variables of Sivagnanam's et al. (1988) sample which exhibit H_2O maser emission (from Benson et al. 1990). The outliers (stars) in the right side are QS Her and V2090 Oph.

is classified as SRb star of $0\overset{\mathrm{m}}{.}7$ photographic amplitude and period of 600 days having a brightness of 12^{m} at maximum (GCVS). V2090 Oph is an optically faint star (15^{m} at maximum) tentatively classified as Lb object due to insufficient variability data (GCVS).

Bessel et al. (1989) argued that the various loci of semiregular variables in the NIR colour-colour diagram are mainly due to effective temperature differences rather than water vapour absorption bands. Because there are no significant differences in the infrared colours between Lb stars of our sample and SRa/SRb stars of the comparison sample the spread of the loci for the irregulars may reflect effective temperature differences as well. In the vicinity of the Mira domain, i.e. around $J-H \sim 1.0$, $H - K \sim 0.5$, almost all objects are maser sources. We note however, a significant scatter in the NIR colours of H_2O maser stars, which suggests that there is only an increasing probability of finding maser emission when the effective temperature of a star decreases.

In order to compare the far-infrared properties and their effect on water maser activity in stars of different pulsational behaviours we compiled another sample consisting of all Me–type Miras selected by Sivagnanam et al. (1988), which have been detected in the water line (Benson et al. 1990). Fig. 6 shows the IRAS [25]−[60] colour versus the $K - [12]$ colour for the sample of Lb variables and the two comparison samples of SRa/SRb variables and Mira stars. The IRAS colour is defined as $[\lambda_1] - [\lambda_2] = -2.5\log(S_\nu(\lambda_1)/S_\nu(\lambda_2))$, where $S_\nu(\lambda)$ is the uncorrected flux density at λ in Jy. In this diagram the SRa and SRb H_2O maser variables are an extension of Mira maser variables towards bluer $K - [12]$ and $[25] - [60]$ colours with partial overlap of both classes. The infrared colours of the irregular stars are the same as those of SRa and SRb stars and

the bluest Miras. The lack of objects with $K-[12] < 1.3$ for both irregular and semiregular variables is due to our selection, as only the reddest objects are studied here. Towards bluer colours there are no water masers at all. For a given $K-[12]$ colour the maser stars are among the objects with the reddest $[25]-[60]$ colours. We did not find any Lb star in our sample, which has infrared properties differing from those of SRa and SRb maser variables. Furthermore, 3 out of 6 maser sources have infrared colours typical for the bluest maser Miras, and QS Her, and V2090 Oph have $K-[12]$ colour of 4.47 and 3.70 respectively, which are not compatible with those of usual irregular and semiregular stars. The location of irregular variables in the infrared colour-colour diagrams suggests effective stellar temperatures and mass loss rates similar to those of semiregular and blue Mira variables. The probability to detect a water maser in an irregular variable increases with lower effective temperatures and higher mass loss rates, as it is found also in the more regularly pulsating stars.

5. Discussion

About 64% stars in our sample is of Lb–type and no accurate method of determining their distances exists. Because a subset of 10 objects in our sample has been observed in the $JHKLM$ bands, the apparent bolometric magnitudes could be calculated by integration of the flux densities in the visual, NIR and IRAS bands. For these objects the energy distributions were well fitted by two blackbody curves and a linear relationship between the apparent bolometric and $K-$band magnitudes could be established. This relation was used to derive the bolometric magnitudes for the remaining Lb stars in the sample from K magnitudes found in Gezari et al. (1993). The bolometric magnitudes were then used to calculate distances by assuming a mean absolute bolometric magnitude of $-4\overset{\mathrm{m}}{.}5$. This magnitude is very close to the bolometric magnitude of oxygen–rich Miras with periods in the interval of $300-400$ days or semiregulars with $100 \leq P < 150$ days, which are thought to be members of the same population as the irregulars (Jura & Kleinmann 1992). Because the sample contains only the reddest irregular variables, similar to the semiregulars and blue Miras, which emit almost all of their energy in the wavelength range 0.7 to 100 μm, we expect that the mean bolometric luminosity of 0.5 $10^4 L_\odot$ (e.g. $M_{\rm bol} = -4.5$) applies to these stars with exception of QS Her and V2090 Oph, for which we assumed a mean bolometric luminosity of $10^4 L_\odot$. The bolometric distances of SRa and SRb stars were estimated as described elsewhere (Szymczak & Engels 1995).

The bolometric distances of Lb variables range from 0.25 to 1.01 kpc and only 27% of them are closer than 0.4 kpc. The distances of QS Her and V2090 Oph are $\sim$1.4 and $\sim$2.9 kpc, respectively. 3 out of 12 Lb variables in the solar vicinity (D$\leq$400 pc) show H_2O maser emission. In the same volume about 28% of 96 SRa and SRb variables from our comparison sample are H_2O maser sources. This shows that the rate of water maser emitting objects in both samples are nearly the same.

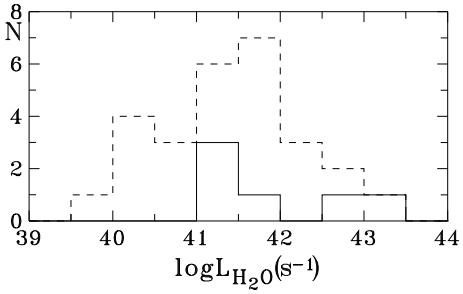

Fig. 7. Distributions of the H_2O maser luminosity of the Lb stars (solid line) with D $\leq$ 400 pc and SRa+SRb variables (dashed line) from the comparison sample.

The water maser luminosities of the Lb stars were calculated using the relation $L_{\rm H_2O}$ = 8.5 $10^{40} S_{\rm i} D^2$, where $S_{\rm i}$ is the integrated flux density in 10^{-22} W m^{-2} and D is the distance in kpc. The maximum value of $S_{\rm i}$ from different epochs was used. The H_2O photon luminosities of the Lb stars range from 1.3 10^{41} to 1.3 10^{43} s^{-1} (Table 3). The median value of 4.7 10^{41} s^{-1} is nearly the same as the one found for SRa and SRb variables (Szymczak & Engels 1995) and is about one order of magnitude smaller than that for local Mira variables (Bowers & Hagen 1984). As noted before, QS Her and V2090 Oph are not included in the above estimate. Although TW Peg was a strong H_2O maser emitter in 1973 (Dickinson 1976), we adopted a current upper limit of $L_{\rm H_2O}$ = 4.0 10^{40}s^{-1} as the star was never detected afterwards (cf. Benson et al. 1990). The distributions of the H_2O maser luminosity of Lb stars and our comparison sample of SRa and SRb variables are shown in Fig. 7. For two Lb objects upper limits of $L_{\rm H_2O}$ were used in this diagram. The lower bounds of both luminosity distributions are due to similar sensitivity limits of the observations. Figure 7 illustrates that the distribution of H_2O luminosity of the sample of Lb sources are comparable to that observed in the comparison sample of SRa and SRb stars, although there are no Lb objects with very low luminosity. This is probably a selection effect only because in the present study we have mostly distant Lb variables ($D >$400 pc), while in the comparison sample nearby SRa and SRb stars ($D <$400 pc) predominate. We conclude that the maser luminosities of the irregular variables do not differ from the luminosities of SRa and SRb stars.

The lack of large differences in the $K-[12]$ colour distribution between the semiregulars of SRa– and SRb–type and Lb objects (cf. Sect. 4.2) suggests that both classes of variables lose mass at no significant different rates. To quantify this parameter we used Jura's (1987) formula: $\dot{M}$ = 1.1 $10^{-8} v_{\rm d} D^2 L_4^{-0.5} S_{60} \lambda_{10}^{0.5}$. Here the dust outflow velocity $v_{\rm d}$ is 10 km s^{-1} and the stellar luminosity L_4, in units of 10^4 solar luminosities, is 0.5. A standard value of 0.15 for the mean wavelength λ_{10} of the whole spectral energy distribution is assumed. D is the distance in kpc and S_{60} is the IRAS flux density at 60 μm. Mass loss rates of the H_2O maser stars are usually higher than $\sim$ 4. $10^{-8} M_\odot$yr^{-1} (Table 3). The average value of $\dot{M}$ = 6.2 $10^{-8} M_\odot$yr^{-1} for Lb maser stars is only slightly higher

Table 3. Properties of irregular and semiregular variables with H_2O maser emission

Name	Var. type	Sp. type	D (kpc)	log L_{H_2O} (s^{-1})	V_e (km s^{-1})	$\dot{M}$ ($10^{-7} M_\odot$ yr^{-1})
T Psc	SRb	M5	0.70	41.7[a]		0.30
CE And	Lb	M2	0.82	43.1	5.8	0.85
RY Ari	Lb	M6.5	0.60	<41.5		0.50
BX Eri	SR	M2−7	0.35	42.5	4.1	0.62
VZ Eri	SR	M3−7e	0.85	42.2		0.39
DW Gem	Lb	M3−7	0.33	41.2		0.64
CW Cnc	Lb	M6	0.30	41.1		0.42
BK Vir	SRb	M7III	0.19	<40.5[a]		0.41
WY Boo	SR	M5	0.71	41.6[a]		0.61
TY Dra	Lb	M5−8	0.42	41.8[a]		0.79
QS Her	SRb	M2	2.87	43.7[b]		17.90
TU Lyr	Lb	M6	0.39	42.7[a]	4.8	0.53
V2090 Oph	Lb:	M6−9	1.39	43.4	13.8	5.68
TW Peg	SRb	M6−8	0.21	<40.6		0.56

[a] unpublished Effelsberg data
[b] Engels & Lewis (1996)

than that of non-maser stars. The lower limit of mass loss rates in irregular maser stars is comparable to that derived for the maser SRa and SRb variables (Szymczak & Engels 1995). The expansion velocities of H_2O masers in Lb stars, deduced from the outer peak separations are 4–6 km s^{-1} (Table 3).

Lane et al. (1987) have found that the mass loss rate sets the outer radius of the water masing region. Recent data on Mira–type and semiregular variables have confirmed a gradual increase of the size of maser region with the mass loss rate (Bowers & Johnston 1994; Yates & Cohen 1994). Because the irregular maser stars have actually the same mass loss rates as estimated for the SRa and SRb maser stars we believe that radii of their maser envelopes do not differ significantly. Bowers & Johnston (1994) found that radii of usually clumped H_2O shells of semiregular and blue Mira variables range from about 5 to 15 AU. Such small shells are expected to emit unsaturated H_2O maser radiation (Reid & Menten 1990). Significant variations of the intensities of total emission and individual features in Lb stars TU Lyr and DW Gem observed at two epochs spanning by about 3 months may be an indirect indication of unsaturated conditions in their shells. Also, the non-detection of some previously known maser stars in our samples suggests that the maser emission is unsaturated.

The relative low probability to detect H_2O masers suggests that the Lb giants sustain maser action at a comparable level as SRa and SRb semiregulars but with lower luminosities as in Miras. It seems that the circumstellar shells of most of the irregular variables in the sample are less developed than those of regular Mira–type stars. The NIR colour–colour diagram (Fig. 5) suggests that irregular variables are more evolved than the red giant branch stars and are at earlier stages than most known asymptotic giant branch (AGB) stars. However, according to Fig. 6 all of them exhibit emission of circumstellar dust as Miras and SRa, SRb variables. One possible explanation is contamination of our sample by unrecognized semiregular and Mira variables. As about half of the selected stars have visual magnitudes ≥ 10 it is likely that their light curves were poorly sampled. Whitelock et al. (1994) provided evidence that a misclassification of some irregulars cannot be ruled out. We found that two sources in our sample are not typical irregulars. A second possibility is that irregulars belong to the same population of mass losing objects as Mira and semiregular variables but have different pulsational properties.

The basic properties of H_2O masers such as luminosity and profile shape suggest that the irregular giants do not differ substantially from the red SRa and SRb variables (Szymczak & Engels 1995). The scale height of irregulars are similar as that estimated for the Miras and semiregulars with periods of 300–400 days and 100–150 days respectively (Jura & Kleinmann 1992). The amount of circumstellar material around some irregulars is high enough to support water maser emission, at least temporarily. If the Lb maser stars really show irregular or weakly pronounced periodic variations of small amplitudes in the optical domain as a result of competition of different pulsation modes (Buchler & Goupil 1988; Jura & Kleinmann 1992), one can presume that they are on the AGB and have undergone very recently a thermal pulse. As a consequence of thermal pulse the regular and high amplitude changes in the light curve were replaced by the presently observed irregular behaviour (Vassiliadis & Wood 1993). This episode is probably associated with a reduction of mass loss rate but to a level which still sustains collisional excitation of water molecules (Cooke & Elitzur 1985). A recent calculation by Vassiliadis & Wood (1993) has shown that several superwind phases on the AGB can occur. However, in their model the relaxation phase after a thermal pulse is very short with regard to the time of evolution on the AGB. For a typical thermal pulse AGB lifetime of 10^5 yr less than 0.2% objects experience a sudden change of their pulsational properties. Thus the above interpretation is poorly consistent with a quite large number of Lb stars. In the GCVS as many irregulars as

semiregulars are listed. Some Lb stars might be misclassified due to poor sampling of their light curves but if the Lb type genuinely exists it is quite abundant. Therefore one can alternatively presume that Lb stars are at the early AGB stage, which lasts a long time, trying to start their pulsations. This seems to be consistent with the moderate infrared excess and weak mass loss of most of irregular variables.

6. Conclusions

We made a survey for H_2O maser emission in 72 irregular and semiregular M-type stars leading to 9 detections, of which 5 were detected for the first time. Our sample was selected from the GCVS and is probably not homogeneous as part of the objects are probably unrecognized Mira variables. This is indicated by the IR and/or maser properties of two of them (QS Her and V2090 Oph). Several objects known to have water maser emission were not redetected. This suggests that the masers are variable as in the case of SRa and SRb variables. The infrared and maser properties of the sample are very similar to those of SRa and SRb variables.

Acknowledgements. The authors would like to thank the Directors of the Max Planck Institute for Radioastronomy for observing time at the Effelsberg radio telescope. The research of MS was supported under grant 2 P 304 004 05 by the Polish Committee of Scientific Research.

References

Benson P.J., Little–Marenin I.R., Woods T.C., et al., 1990, ApJS 74, 911
Bessell M.S., Brett J.M., Scholz M., Wood P.R., 1989, A&A 213, 209
Bowers P.F., Hagen W., 1984, ApJ 285, 637
Bowers P.F., Johnston K.J., 1994, ApJS 92, 189
Buchler J.R., Goupil M.J., 1988, A&A 190, 137
Cooke B., Elitzur M., 1985, ApJ 295, 175
Dickinson D.F., 1976, ApJS 30, 259
Engels D., Lewis B.M., 1996, A&AS 116, 117
Fouqué P., Le Bertre T., Epchtein N., Guglielmo F., Kerschbaum F., 1992, A&AS 93, 151
Gezari D.Y., Schmitz M., Pitts P.S., Mead J.M., 1993, Catalog of Infrared Observations, NASA RP–1294
IRAS Science Team, 1988, IRAS Catalogs and Atlases, Volume 1: Explanatory Supplement, NASA RP–1190
IRAS Science Team, 1986, IRAS Catalogs and Atlases, IRAS Atlas of low–resolution Spectra, A&AS 65, 607
Jura M., 1987, ApJ 313, 743
Jura M., Kleinmann S.G., 1992, ApJS 83, 329
Kerschbaum F., Hron J., 1994, A&AS 106, 397
Kholopov P.N., Samus N.N., Frolov M.S. et al., 1985–88, General Catalogue of Variable Stars, 4th ed., Moscow (GCVS)
Lane A.P., Johnston K.J., Bowers P.F., Spencer J.H., Diamond P.J., 1987, ApJ 323, 756
Lewis B.M., Engels D., 1993, MNRAS 265, 161
Reid M.J., Menten K.M., 1990, ApJ 360, L51
Sivagnanam P., Le Squeren A.M., Foy F., 1988, A&A 206, 285
Szymczak M., Engels D., 1995, A&A 296, 727
Szymczak M., 1996, In: Radio Emission from the Stars and the Sun, eds. R.A. Taylor & J.R. Paredes, ASP Conf. Series vol. 93, 116
Vassiliadis E., Wood P.R., 1993, ApJ 413, 641
Whitelock P., Menzies J., Feast M., Marang F., Carter B., Roberts G., Catchpole R., Chapman J., 1994, MNRAS 267, 711
Whitelock P., Menzies J., Feast M., Catchpole R., Marang F., Carter B., 1995, MNRAS 276, 219
Yates J.A., Cohen R.J., 1994, MNRAS 270, 958

This article was processed by the author using Springer-Verlag LaTeX A&A style file *L-AA* version 3.